



# Decadal re-forecasts of glacier climatic mass balance

Larissa Nora van der Laan<sup>1,2</sup>, Anouk Vlug<sup>3,4</sup>, Adam A. Scaife<sup>5,6</sup>, Fabien Maussion<sup>4,7</sup>, and Kristian Förster<sup>8,2</sup>

<sup>1</sup>Niels Bohr Institute, University of Copenhagen, Copenhagen, Denmark

<sup>2</sup>Institute of Hydrology and Water Resources Management, Leibniz University Hannover, Hannover, Germany

<sup>3</sup>Institute of Geography, University of Bremen, Bremen, Germany

<sup>4</sup>Department of Atmospheric and Cryospheric Sciences, University of Innsbruck, Innsbruck, Austria

<sup>5</sup>Met Office Hadley Centre, Exeter, UK

<sup>6</sup>College of Engineering, Mathematics and Physical Sciences, University of Exeter, Exeter, UK

<sup>7</sup>Bristol Glaciology Centre, School of Geographical Sciences, University of Bristol, Bristol, UK

<sup>8</sup>Institute of Ecology and Landscape, University of Applied Sciences Weihenstephan-Triesdorf, Freising, Germany

**Correspondence:** Larissa Nora van der Laan ([larissa.vdlaan@nbi.ku.dk](mailto:larissa.vdlaan@nbi.ku.dk))

**Abstract.** We present the first study using decadal re-forecasts to simulate global glacier climatic mass balance, bridging the gap between seasonal and long-term simulation of glacier contribution to catchment hydrology and sea level rise. Using the Open Global Glacier Model, driven by Coupled Model Intercomparison Project 6 ensembles of initialised decadal climate re-forecasts of temperature and precipitation, we demonstrate the skill of glacier mass balance re-forecasts on the decadal timescale, for respectively 279 reference glaciers and all land-terminating glaciers globally. For comparison, the glacier model is also forced with a simple persistence forecast and general circulation model historical time series and projections, representing the current state of the art. The results from forcing with decadal re-forecasts provide improvement over the other two methods. Simulating single years, especially at short lead times, decadal re-forecasts show the highest Pearson correlations and lowest mean absolute errors, compared to observed mass balance. Simulating cumulative mass balance over full decades for the 279 reference glaciers, forcing with decadal re-forecasts yields a decrease in mean absolute error of 18 % and 16 % compared to forcing with persistence forecasts and historical global circulation model simulations, respectively. Globally, comparing average mass balance over the time period 2000–2020, forcing with decadal re-forecasts results in the highest number of regions with 'good fit' to observations (difference from observed regional mass balance  $\leq 0.1$  m w.e.), compared to the persistence and historical climate model forcing. These findings indicate that the use of decadal predictions for glacier modelling is operationally feasible and holds significant potential for future hydrological applications.

## 1 Introduction

As unique indicators of climate change, water storage reservoirs and culturally significant sites, glaciers serve a multitude of purposes (Allison, 2015; Bosson et al., 2019; Farinotti et al., 2020; Jansson et al., 2003). Observing and simulating their response to climate change on various time scales, from millennia to a focus on the past century, is an essential and continuously developing field of study (e.g. Goosse et al. (2018); Hock et al. (2019); Malles and Marzeion (2021); Marzeion et al. (2017); Roe et al. (2021); Vargo et al. (2020)). While the storage outside the Greenland and Antarctic Ice Sheets only constitutes a



small percentage of total global freshwater storage in ice, it is equivalent to approx. 0.32 m of sea level rise (Farinotti et al., 2019). Since these smaller ice bodies respond fastest to changes in the climate, glaciers were the largest contributor to sea-level rise for most of the past century, overtaken by thermosteric contribution after 1970, and are expected to remain a significant contributor in the foreseeable future (Frederikse et al., 2020; Slangen et al., 2017).

Water is accumulated and released by glaciers on various time scales, ranging from long-term storage in ice and firn to short-term storage in snow cover. Within their basins, glaciers act as a buffering system, preventing precipitation from immediately turning into runoff in downstream rivers (Jansson et al., 2003). The seasonality of glacier runoff therefore modulates downstream flow, providing meltwater in otherwise potentially dry seasons or years of low flow (Huss and Hock, 2018; Ultee et al., 2022; Förster and van der Laan, 2022). Due to this buffering capacity, they are essential parts of global water towers, defined as mountain range water storage and supply to downstream communities and ecosystems, upon which 22 % of the global population is dependent for their water needs (Immerzeel et al., 2020).

With changes in climate, glacier mass balance – a temporal integration of both accumulation and melt, largely governed by temperature and precipitation – is altered, impacting over time the glacier mass and thus storage capacity. Decadal time scales are rarely considered in glacier modelling studies, even though they are critical time scales for water resource management, anticipating glacier change induced impacts on catchment hydrology (Frans et al., 2016; Lane and Nienow, 2019). The need for annual to decadal predictions is well recognized, despite the developmental stage of the field (Boer et al., 2016; Merryfield et al., 2020). When using the term decadal in this study, it encompasses time scales of one to ten years. The term “decadal prediction”, as used here, encompasses predictions on annual, multi-annual and decadal timescales (Boer et al., 2016).

In 2016, the World Climate Research Programme (WCRP), co-sponsored by the World Meteorological Organisation (WMO), the Intergovernmental Oceanographic Commission (IOC) of UNESCO, and the International Science Council (ISC), set up the Grand Challenge on Near Term Climate Prediction, to make the case for, and understand the challenges in establishing routine operational climate predictions on these time scales (Kushnir et al., 2019). As of now, there are multiple ensembles of model hindcasts/re-forecasts available. These terms are used interchangeably in literature. In this study, for consistency, we will use the term re-forecast, defined here as a retrospective prediction (Boer et al., 2016), realised with the aim to evaluate them against observations and provide insight into our capacity of providing real decadal forecasts.

With the advent of operational predictions (Hermanson et al., 2022), there is growing research activity in applications (Dunstone et al., 2022). Glacier modelling is one such field, where there is a gap between seasonal modelling of glacier mass balance and runoff (e.g. Koziol and Arnold, 2018; Réveillet et al., 2018), and the more established modelling on the century and millennial scale, often using downscaled general circulation model (GCM) output (e.g. Huston et al., 2021; Rounce et al., 2023). By quantifying and improving the predictability of glacier mass balance on the decadal scale it may be possible to bridge this gap. If so, the resulting mass balance predictions could also be translated into glacier runoff, serving as an important input for water resource decisions, which often operate on this time scale (Kiem and Verdon-Kidd, 2011).

The aim of this study is to investigate the utility of forcing a mass balance model with decadal scale re-forecasts, to complement current mass balance modelling studies and the time scales they are commonly conducted on. As far as we know, this study is the first of its kind in large scale glaciology, following suit to testing the applicability of decadal re-forecasts in



60 impact models for other research disciplines, such as marine biology (Payne et al., 2022) and the agricultural sector (Solaraju-Murali et al., 2022). A compacted review of applications, including a preliminary version of the current study, is presented in O’Kane et al. (2023). In the current manuscript, we present a global modelling approach using the Open Global Glacier Model (OGGM: Maussion et al., 2019), forced with a multi-model, multi-member retrospective ensemble of monthly temperature and precipitation re-forecasts from the Coupled Model Intercomparison Project Phase 6 (CMIP6) Decadal Climate Prediction Project (DCPP: Boer et al., 2016). In order to assess whether decadal forcing provides added skill, we compare them with simulations where OGGM is forced with a simple persistence method and with uninitialized, free running historical GCM output and projections from the same models (i.e. the traditional forcing approach for 21<sup>st</sup> century simulations).

## 65 2 Data and Methods

### 2.1 Model

We use OGGM v.1.5.3 (Maussion et al., 2019) for the first component of the study – the simulation of reference glaciers – and a slightly updated version, in terms of calibration, for the global runs, which was not an official release (see Sect. 2.2.2). OGGM is an open-source modeling framework written in Python. It was developed to provide a catchment to global-scale, modular numerical modeling framework for various study set-ups of glacier evolution on multiple scales, while accounting for glacier geometry and ice dynamics. Maussion et al. (2019) and the continuously expanding and adapting model documentation at <http://docs.oggm.org> explain the model in detail and can be referred to for the in-depth model description. The current study focuses on the application of the model and will thus only give a brief overview and introduce the relevant components, including more detailed information on the mass balance models being used.

#### 75 2.1.1 Workflow

The model takes a glacier-centric approach, using the outline of a glacier as a starting point. By default, the glacier outlines are automatically taken from the Randolph Glacier Inventory (RGI) version 6.0 (Pfeffer et al., 2014; RGI Consortium, 2017). Given a glacier outline and topographical and climate data, OGGM aims to: “i) provide a local map of the glacier including topography and hypsometry, (ii) estimate the glacier’s total ice volume and compute a map of the bedrock topography, (iii) compute the surface climatic mass balance and (if applicable) its frontal ablation, (iv) simulate the glacier’s dynamical evolution under various climate forcings and (v) provide an estimate of the uncertainties associated with the modelling chain” (Maussion et al., 2019; Recinos et al., 2019). In this study, we solely use the pre-processing and mass balance modelling capabilities of the model, not the glacier dynamics. We call this “fixed geometry”, i.e. the surface area and elevation of the glacier are fixed when computing glacier wide mass balance. Our assumption is that geometry feedbacks are not too important at the annual and decadal scales and are overshadowed by other uncertainties (such as the unknown glacier state in the past, e.g. Eis et al. (2021)). Furthermore, we only evaluate the climatic mass balance component and do not evaluate calving or other mass loss processes: from now on, we will use the term “mass balance” in place of “climatic mass balance” for simplicity.



## 2.1.2 Mass Balance

The mass balance module selected for the model set-up is the OGGM default as of 1.5.3. Mass balance is calculated using a  
90 temperature index model which generates monthly accumulation and ablation along the glacier:

$$m_i(z) = p_f P_i^{solid}(z) - \mu^* \max(T_i(z) - T_{melt}) + \epsilon, \quad (1)$$

in which  $m_i$  is monthly mass balance at elevation  $z$ ,  $T_i$  constitutes the monthly temperature that is adjusted based on its elevation by using a temperature lapse rate of  $6.5 \text{ K km}^{-1}$ .  $T_{melt}$  is the monthly mean temperature threshold (default of  $-1^\circ\text{C}$ ) above which melt occurs.  $p_f$  is a precipitation correction factor, here set to 2.5 globally (Maussion et al., 2019).  $P_i^{solid}$   
95 is the monthly solid precipitation, computed as a fraction of total precipitation, based on the monthly mean temperature. The temperature sensitivity of a glacier is indicated by calibrated parameter  $\mu^*$ , and  $\epsilon$  is an optional residual, determined during calibration. In this study we make use of two independent calibration procedures, one making use of observations of glaciers with a mass balance record of at least five consecutive years (Sect. 2.2.1) and the other being based on a global dataset (Sect. 2.2.2).

## 100 2.2 Mass Balance Model Calibration

### 2.2.1 Calibration with WGMS Data

For the first component of the study, the mass balance calibration procedure is carried out with baseline climate CRU, see Sect. 2.4, and direct observations from the World Glacier Monitoring Service (WGMS,  $N = 279$ ) (WGMS, 2022). For these glaciers, referred to as reference glaciers, we use the default calibration procedure as of OGGM 1.5.3, described in Marzeion et al.  
105 (2012) and Maussion et al. (2019). For all years with observations, the model output is then compared to observations, arriving at the best candidate(s) for  $\mu^*$  and  $\epsilon$ . For this part of our study, the focus is on the 279 land-terminating WGMS glaciers, therefore the parameters do not need to be transferred to glaciers without observation and are therefore well constrained.

### 2.2.2 Calibration with Geodetic Data

For the global component of this study, OGGM benefits from the dataset by Hugonnet et al. (2021), providing geodetic mass  
110 balance estimates for 94 % of the number of global glaciers. The monthly mass balance is computed as in Eq. (1) but without making use of the residual  $\epsilon$ , since this dataset allows the calibration with individual glaciers. The calibration is again done for temperature sensitivity parameter  $\mu^*$ , calibrated to match the glacier's geodetic mass balance of the period 2000–2020; the reference period in Hugonnet et al. (2021). If this results in an unrealistic  $\mu^*$ , bound by a pre-defined range (here:  $50$  to  $600 \text{ kg m}^{-2} \text{ K}^{-1}$ ), the reference temperature time series are bias corrected until this results in a physically realistic  $\mu^*$ . Note that  
115 the re-calibration for the global run is a practical necessity (we are simulating all glaciers globally) but has no bearing for our results, since we compare OGGM results with different forcing strategies, i.e. we are not assessing the model or its parameters but the forcing data used for the simulations. It must be added that in our study, we will always run the model during the period



it has been calibrated for. This means that when run with the baseline climate CRU, it provides perfect results when compared to observations over the calibration period (mean bias of zero).

### 120 2.2.3 Experiments

In this work, we carry out three separate forcing experiments with OGGM. The focus of the study is on decadal re-forecasts, but in order to put the results into context we perform two additional experiments which represent forecasting from very simple to complex. In the first component of all experiments we run OGGM's mass balance model, calibrated with direct mass balance observations, for all land-terminating WGMS reference glaciers ( $N = 279$ ), over the period 1990–2020. The geometry of the glacier is based on the state at the RGI inventory date, usually between the years 2000 and 2010, and remains unchanged throughout the simulation.

These experiments are repeated for the second component in a global set-up that uses the mass balance model calibrated for each land-terminating glacier globally, against geodetic mass balance data (see Sect. 2.2.2). Here, the mass balance of the approximately 214,000 land-terminating glaciers is simulated over the period 1990–2020. In all experiments, validation is carried out over the period 2000–2020.

The experiments are defined as follows:

**1) Decadal re-forecast:** OGGM run 1990–2020, forced with a 21 member multi-model ensemble of CMIP6 DCP-A decadal re-forecasts (see Sect. 2.4 and Table 1). All different realizations (ensemble members) are downscaled to the glacier scale and run for all available decades.

135 *Final output:* a set of ensemble means of results, according to the methodology in Sect. 2.5.

**2) Persistence:** OGGM run 1990–2020, forced with a simple, persistence-type forecast. Persistence forecasts are a typical null hypothesis against which other forecast skill is measured (Hargreaves, 2010). Here, each period (lead times 1 to 9 years, see Sect. 2.3) is the same as the one that precedes it (from here on referred to as 'persistence forecast'). For this, we use baseline climate CRU.

140 *Final output:* per lead time, one time series with one mass balance value per year and glacier, from the simulation with the baseline climate.

**3) GCM Historical:** OGGM run 1990–2020, forced with a 21-member ensemble of CMIP6 historical simulations, using climate projections for 2014–2020, see Sect. 2.4. Historical GCM runs and GCM projections are the current state of the art in forcing glacier models for the 20<sup>th</sup> and 21<sup>st</sup> century, including on the near-term time scale (see Hock et al., 2019, Slangen et al., 2017 and Zekollari et al., 2022 for overview papers).

145 *Final output:* a multi-model ensemble mean of results, from averaging results of the simulations with each of 21 members. This yields a time series with one mass balance value per year and glacier.



The purpose of this combination of experiments is to assess the added value of the decadal re-forecasts over a naïve forecast method (persistence) and current state of the art (GCM historical), as well as analyze forecast skill of decadal and persistence (re-)forecasts at different lead times.

### 2.3 Lead Time and Ensembles

Due to the importance of the initial state for decadal prediction, forecast skill often declines with lead time (Zhu et al., 2019). Lead time here adheres to the definition by the American Meteorological Society: “*The length of time between the issuance of a forecast and the occurrence of the phenomena that were predicted*”. To assess the lead time based skill in the context of our study, we create lead time based ensemble means of results in the decadal re-forecast experiment, to validate against observations. This results in nine time series of mass balances, 2000–2020, with input from lead times 1-9, respectively. Due to the clipping to hydrological years to match the WGMS measurements, lead time 0 does not exist. So for a decadal re-forecast initialized in 1990 (always in November), the first full year of simulated values is for the year 1992.

For the persistence experiment, we also create lead time based time series. Here, lead time refers to the forecast length, which is the same time period until the start of the forecasts. An example of lead time 2 would be the year 2000-2001 being the same as the year 1998-1999. In the case of our study period 2000–2020, the lead time 1 persistence forecast uses temperature and precipitation from the time period 1999-2019, and lead time 9 utilizes values from 1991-2011 for the forecast. Finally, in our decadal re-forecast experiment, we create ensemble means of results as they would be utilized in practice. As Risbey et al. (2021) note, many assessments of re-forecast skill are likely overestimated, as the re-forecasts are informed by observations over the period assessed that would not be available to real forecasts. In order to avoid this as much as possible, we only assess a period that was not used in the drift correction and use only lead times that would be available at the beginning of the forecast period. This results in time series for each glacier and each full decade in the period 2000–2020. For an example decade, say 2000-2010, the ensemble mean of results consists of information from all re-forecasts initialized in 1990–2000. This means the ensemble size decreases over time, with only lead time 9 information being available in 2009. We use information from all lead times available to maximize ensemble size, and in turn skill (Kadow et al., 2017). This approach again re-iterates the fact that decadal re-forecasts are multi-annual, rather than strictly ten years. In order to compare persistence as it would be used in practice, for decadal mean and cumulative mass balance forecasting, persistence forecasts at lead time 9 are applied.

### 2.4 Climate Data

The mass balance model in OGGM requires monthly climate in the form of reference height (2 m) temperature and precipitation time series. We use the gridded Climatic Research Unit Time Series (CRU TS4.01) (Harris et al., 2014) as the past climate reference dataset. This coarse (0.5°) dataset is then interpolated to a higher resolution climatology (CRU CL v2.0 at 10' resolution New et al., 2002) following the anomaly mapping approach described in Harris et al. (2020), to acquire climate time series with elevation data, which is not an attribute in the CRU TS. For each glacier, the monthly time series of temperature and precipitation are taken from the gridpoint closest to the glacier. Temperature is converted using an elevation-based lapse rate of 6.5 K km<sup>-1</sup> and precipitation is corrected using the default correction factor of  $p_f = 2.5$ . We use CRU for our persistence





experiments. While the CRU dataset constitutes our OGGM baseline climate for calibration, OGGM can also be supplied with GCM output that is bias corrected to the baseline climate, as we do in the decadal re-forecast and GCM historical experiments.

In the decadal re-forecast experiment, OGGM is driven with a multi-model, multi-member retrospective ensemble of monthly temperature and precipitation re-forecasts from the DCP component A, which provides re-forecasts. We use decadal  
185 realizations from the ‘Flexible Global Ocean-Atmosphere-Land System Model’ (FGOALS Zhou et al., 2018), the ‘Norwegian Climate Prediction Model’ (NorCPM Counillon et al., 2016; Bethke et al., 2021) and the ‘Model for Interdisciplinary Research on Climate version 6’ (MIROC6 Tabebe et al., 2019; Kataoka et al., 2020). We use the r1i1p1f1-r1i1p1f10 realization of all models, where available, see Table 1 for a summary of the full multi-model ensemble. The decadal re-forecasts are initialized each year in the period 1960–2010, the first forecast year being 1961, of which we use years 1990–2010. The processing of the  
190 decadal data is explained below, in Sect. 2.5.

In the GCM historical experiment, we drive OGGM with temperature and precipitation from the historical iteration and projections of the same three GCMs, obtained from CMIP6 archived model output: FGOALS, NorCPM and MIROC6 (see Table 1). The end of the historical simulation is in 2014 and data from 2015–2020 is provided by projection runs, leading to 11 full decades in the period 2000–2020. As the amount of available data becomes larger because of the different shared socio-  
195 economic pathways (SSP), the choice is to select certain SSPs or to introduce a discrepancy in ensemble size, if using all CMIP6 SSPs. We realize that neither option facilitates perfect comparison with the decadal re-forecast and persistence experiment. However, the benefit of comparison with projections outweighs these concerns, as initialized forecast vs. projections represents the most realistic future use case. To preserve ensemble size, SSP245 was chosen as the projection for comparison, as it represents a medium pathway of future greenhouse gas emissions. From FGOALS runs, not enough SSP245 realizations were  
200 available at the time of the study, so SSP126, SSP245 and SSP585 time series were used. As these scenarios do not diverge significantly during 2015–2020, we still consider these results comparable.

In the pre-processing for this experiment, the time series are bias-corrected and downscaled to the glacier scale using a variation of the delta method (Ramírez Villegas and Jarvis, 2010). Here, we take GCM anomalies relative to the 1961–1990 GCM mean for temperature and apply these to the CRU TS 4.01 (Harris et al., 2020) 1961–1990 means. The correction is  
205 applied monthly and ensures that mean and standard deviation are preserved during the bias correction period for temperature. Precipitation is corrected with a multiplicative factor and preserves only the mean. This is the standard method of processing GCM data for projection studies, (e.g. Zekollari et al., 2020), and is the reason we use it as an evaluation procedure for the decadal re-forecasts.

## 2.5 Re-Forecast Drift Correction and Downscaling

210 As is inherent to modelling, the re-forecasts used here contain differences between modelled and observed climatologies, referred to as biases, needing to be corrected. In order to drive OGGM with the re-forecasts, each member is bias corrected and downscaled to the glacier scale using a statistical method applied with baseline climate CRU (New et al., 2002; Harris et al., 2014). Boer et al. (2016) recommend an overarching bias correction method, regardless of the initialization type. We correct model drift with a method based on recommendations and methods in Boer et al. (2016); Kharin et al. (2012) and



**Table 1.** Decadal Re-Forecast Systems

Model	Full Name	Ensemble Size	Primary Publication
FGOALS	Flexible Global Ocean-Atmosphere-Land System Model	3	(Zhou et al., 2018)
NorCPM	Norwegian Climate Prediction Model	10	(Counillon et al., 2016; Bethke et al., 2021)
MIROC6	Model for Interdisciplinary Research on Climate version 6	8	(Tatebe et al., 2019; Kataoka et al., 2020)

215 Hossain et al. (2022), based on the assumption that the bias contained in each member is model and lead time dependent. Because of our assumption that the bias is different at and dependent on each lead time, subtracting a mean drift would lead to over-compensation at some lead times, and residual drift at others. For this reason, we create lead-time based climatologies, meaning one climatology over 1971-2000 which contains all lead time 1 years from the re-forecasts, one which contains all lead time 2 years, and so on. These are then used to create anomalies relative to the baseline climate. For each model, each  
220 member is bias corrected according to:

$$d_t = \overline{T'_t} - \overline{CRU_{cl}}, \quad (2)$$

$$T'_{m,t,y} = T_{m,t,y} - d_t \quad (3)$$

In which  $d_t$  is the average model bias or drift at each lead time  $t$ , calculated relative to the baseline climate input CRU.  $CRU_{cl}$  is the CRU monthly climatology averaged over 1971-2000 (Harris et al., 2014; New et al., 2002).  $T'_t$  is the model  
225 climatology at lead time  $t$  calculated by averaging the lead time  $t$  re-forecasts of all ensemble members of one model falling into the period 1971-2000.  $T_{m,t,y}$  is the raw re-forecast, of member  $m$  at lead time  $t$  and for year  $y$ .  $T'_{m,t,y}$  is the bias corrected re-forecast of member  $m$  at lead time  $t$  and for year  $y$ . The OGGM output used for validation spans the years 2000–2020 for both the reference glacier and global runs.

### 3 Results and Discussion

#### 230 3.1 Reference Glaciers

We compare the output yielded from the three OGGM experiments (decadal re-forecast, persistence and GCM historical) to both individual observations of glacier mass balance (N = 2676) and mean mass balances over whole decades. We first focus





on individual years, assessing how skill changes with lead time. To quantify model skill, we calculate the mean absolute error and the Pearson correlation coefficient for each lead time based ensemble, with the results displayed in Fig. 1. For the decadal re-forecast experiment, results over individual years show a mean absolute error of 0.64 m w.e. at lead time 1 and 0.65 m w.e. at lead time 9. Pearson correlation is 0.14 and 0.07 at lead times 1 and 9, respectively, both values signifying a low degree of correlation. This indicates that skill is not high when simulating individual years, which is expected, and in line with other studies using OGGM for this set of reference glaciers. One example is Eis et al. (2021), who yield a mean absolute error of 0.60 m w.e. with baseline climate CRU, over the time period from 1917 until the RGI outline date per glacier (often early 2000s).

In terms of decadal re-forecast skill declining with lead time, the mean absolute error stays remarkably consistent, only lowering slightly to 0.63 m w.e. at lead time 4. This is less so the case for the persistence experiment, where mean absolute error oscillates, but ultimately rises from 0.69 m w.e. at lead time 1 to 0.72 m w.e. at lead time 9. For the Pearson correlation, we see a decrease with lead time more clearly, in both experiments, with again a higher oscillation in the persistence forecast. The comparable skill scores, especially at short lead times (1-3 years) mainly reflect the general inability of a simple mass balance model to reliably simulate individual mass balance years. As there is no application of lead time to the GCM Historical experiment, its results are plotted as a constant, to compare the skill score magnitude. Simulating single year mass balances is not the focus of this study, however, these results show that already on the single year level, the results from forcing OGGM with decadal re-forecasts outperform results from the persistence and the GCM historical experiments, which both show higher errors and lower correlations.

Next, we compare mean and cumulative mass balance over full decades, as illustrated in Fig. 2 and Table 2. In the time period 2000–2020, we have 11 full decades for which the mean and cumulative mass balance are calculated per glacier, only using simulated data where observations exist as well.

In all experiments, simulated and observed mean decadal mass balances correspond well, with a model error of  $<0.2$  m w.e.. The persistence experiment shows the largest discrepancy between observed and modelled mean mass balance. Fig. 2 shows the 1:1 skill between observed and simulated mean mass balances for all full decades, for all experiments. In this figure, a clear overestimation of mass balance in the persistence experiment can be noticed: all plot points of the persistence experiments skew left of the line of equality, while the plot points for the other experiments gather around it. The larger error for the persistence experiment is due to the ten-year lag of warming. This illustrates the difficulty of using persistence forecasts at longer lead times, especially when the impact model and thus simulated entity is sensitive to warming, as is the case with glacier mass balance.

The skill differences between the experiments are further quantified in Table 2. Here is evidenced that for the reference glaciers, forcing with decadal re-forecasts outperforms forcing with persistence forecasts or historical GCM data, even though the absolute improvements in skill are small. The decrease in mean absolute error between the persistence and decadal experiment is most significant, with a reduction in mean absolute error of 26 % for the decadal mean values. The error reduction between GCM historical and decadal forcing only constitutes a 7 % reduction in mean absolute error for the decadal means. Skill differences when looking at cumulative decadal mass balance are slightly larger, with mean absolute error reductions of

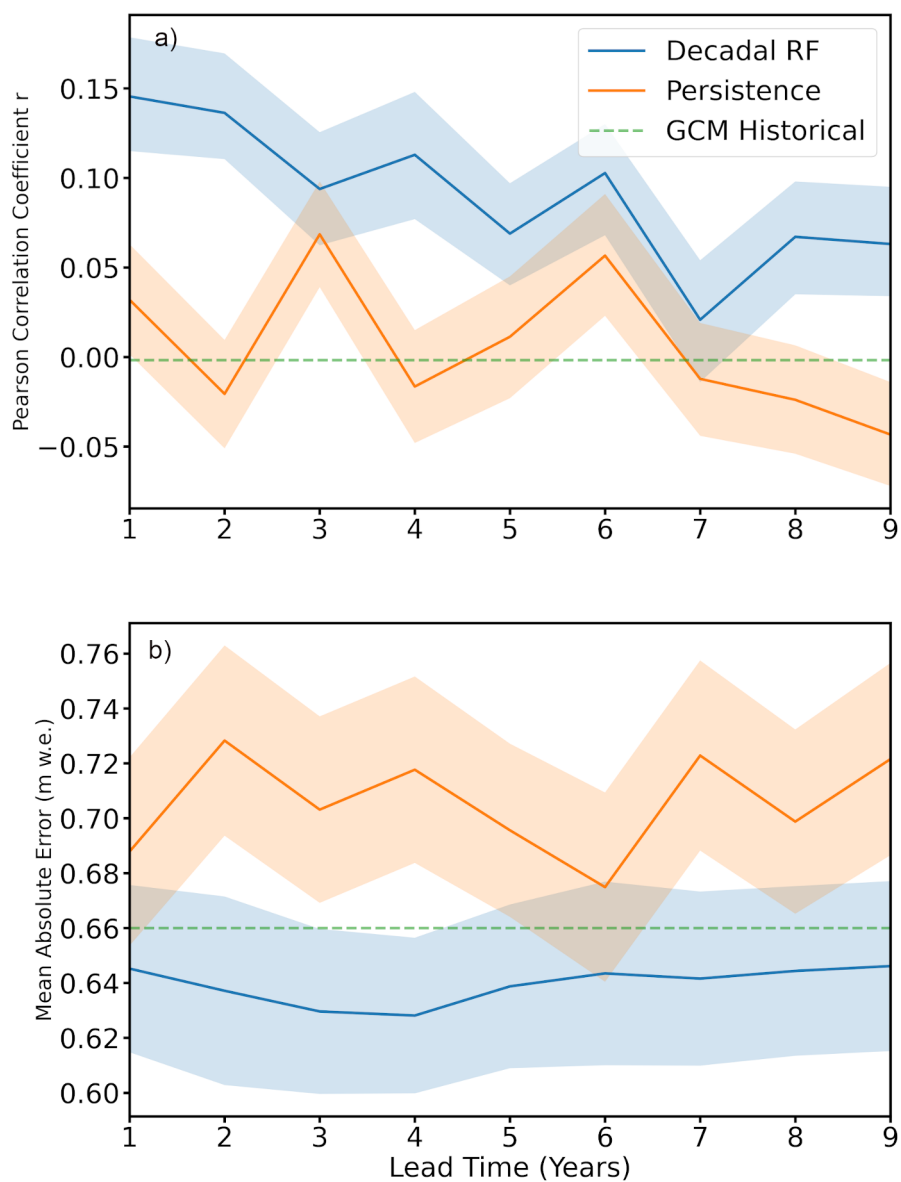


**Figure 1.** Forecast skill for annual mean mass balance for WGMS reference glaciers ( $N = 279$ ). Forecast skill is given as the Pearson correlation coefficient ( $r$ ) and mean absolute error (MAE, m w.e.) between observed and simulated mass balances ( $N = 2676$ ). Skill is plotted as a function of lead time into the future calculated across the appropriate comparison periods (2000–2020) for the decadal re-forecasts and persistence forecasts. The mean skill scores of the GCM historical (2000–2020) simulations also shown for reference, as a constant, since there is no application of lead time. Shaded areas for both persistence and decadal re-forecast (RF) denote the 90 % confidence interval estimated by bootstrapping: 5 % of the distribution is therefore above and 5 % below the shaded areas.

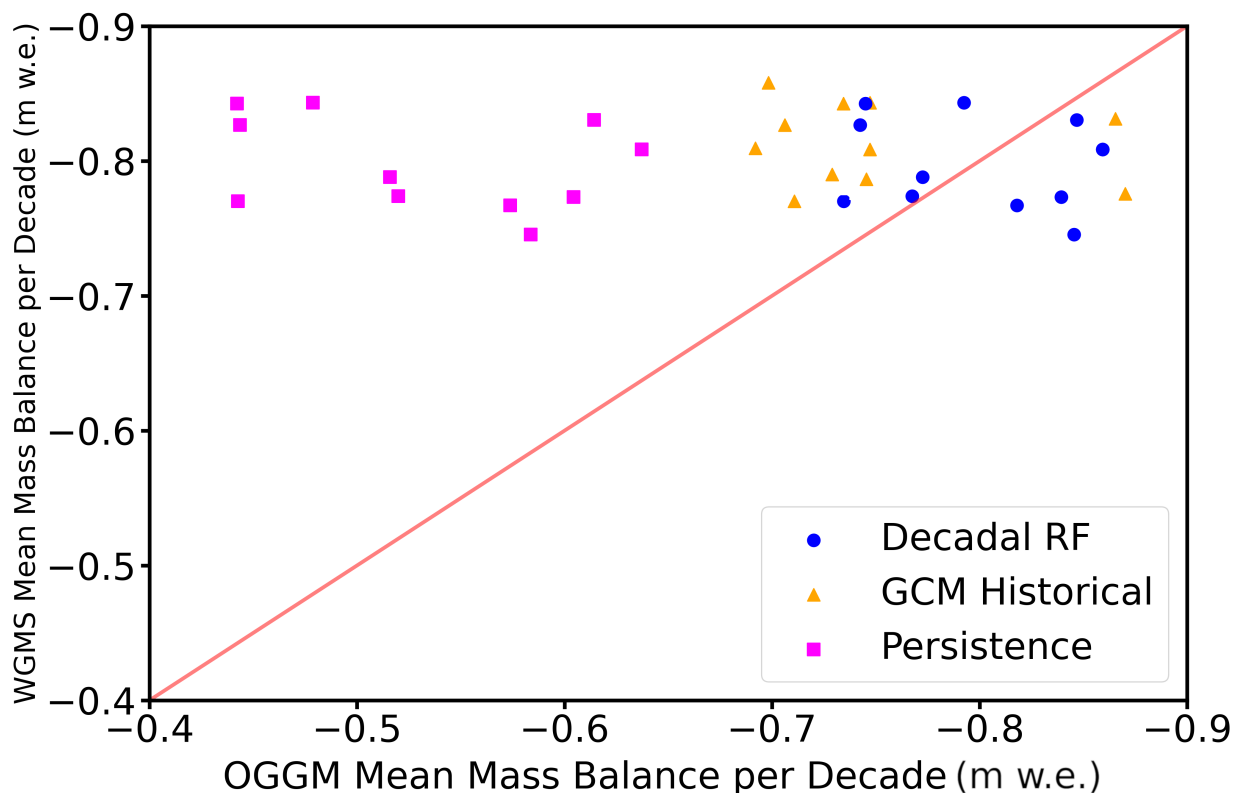


**Figure 2.** Simulated and observed mean mass balances over each full decade ( $N = 11$ ), over all 279 reference glaciers. Only simulated values where observed values are available are used to generate the decadal means.

18 % and 16 % between the decadal re-forecast and persistence and GCM historical experiment, respectively. Pearson correlation coefficients between simulated and observed values are generally in the same range for all three experiments, with highest correlations for the decadal re-forecast experiment. All Pearson correlations are moderate for mean decadal mass balance, up to 0.64 for the decadal re-forecast experiment, and high - up to 0.85 - for cumulative decadal mass balance. Comparing these correlations to the low degree of correlation when simulating individual years emphasizes how the skill of our experiments lies primarily in simulating multi-annual averaged or cumulative mass balances, filtering out inter-annual noise. This is in line with similar approaches, where skill is found through integrating of fluxes over time, such as in seasonal snow accumulation (Förster et al., 2018).

We also note here that in the decadal re-forecast experiment, the multi-model ensemble mean of results yields higher skill than single-model ensembles. Comparing the multi-model ensemble mean of results to observations of mean decadal mass balance vs. single model ensemble means of results ( $N = 3$ ) to observations, yields a decrease in mean absolute error of 11



**Table 2.** Summary of the comparison between WGMS observed and simulated mass balances for all three experiments and the decades 2000-2010 and 2010-2020. The statistics shown are ME: model error, MAE: mean absolute error and Pearson correlation, as well as 1 standard deviation from the mean of the particular statistic.

Skill Measure	Decadal RF	Persistence	GCM Historical
Decadal Mean Mass Balance			
ME (m w.e.)	$0.091 \pm 0.43$	$-0.16 \pm 0.45$	$-0.0059 \pm 0.41$
MAE (m w.e.)	$0.29 \pm 0.32$	$0.39 \pm 0.35$	$0.27 \pm 0.31$
Pearson $r$	$0.64 \pm 0.18$	$0.58 \pm 0.19$	$0.61 \pm 0.22$
Decadal Cumulative Mass Balance			
ME (m w.e.)	$-0.39 \pm 2.50$	$-0.96 \pm 2.74$	$-0.27 \pm 2.26$
MAE (m w.e.)	$1.33 \pm 3.21$	$1.62 \pm 2.46$	$1.58 \pm 2.96$
Pearson $r$	$0.85 \pm 0.08$	$0.74 \pm 0.11$	$0.79 \pm 0.12$

280 % (vs. FGOALS), 8 % (vs. NorCPM) and 6 % (vs. MIROC6), respectively. This is in line with our expectations from the literature, due to an increase in ensemble size and associated error cancellation and the separate forecast systems adding signal to the multi-model ensemble (Kadow et al., 2017; Delgado-Torres et al., 2022). Other studies applying multi-model ensembles in impact model, such as Payne et al. (2022), also come to the conclusion that a multi-model ensemble generally gives the best performance, which is why we do not explore single-model ensemble performance further.

### 3.2 Global Glaciers

285 For all global land-terminating glaciers, we again compare the multi-model ensemble mean of results per decade (see Sect. 2.3) with results from the persistence and GCM historical experiments. To assess skill, 2000-2010 and 2010-2020 results are validated against the global geodetic mass balance dataset by Hugonnet et al. (2021). Because the time period 2000–2020 is covered by both validation datasets, a separate comparison of the two is provided in Sect. 3.3.

290 Analyzing 2000-2010 decadal re-forecast skill scores to the persistence and GCM historical experiments, improvement in skill is slight but clearly noticeable (Table 3). Decadal re-forecast results show smaller errors – a mean absolute error improvement of 23 % and 18 % from persistence and GCM historical forcing, respectively – and higher Pearson correlation, indicating higher skill for re-forecasts, also on the global scale. Over the period 2000-2010, the mean absolute error and standard deviation, calculated over the simulated and observed mean specific mass balance for each single glacier, is  $0.28 \pm 0.23$  m w.e. with the re-forecasts,  $0.35 \pm 0.26$  m w.e. for the persistence forecast and  $0.33 \pm 0.25$  m w.e. in the GCM historical experiment.

295 Between the different glaciated regions of the world - RGI regions, see Fig. 3, there is considerable variation in skill. Indicated in the histograms in Fig. 4 are the regional mean absolute errors for 2000-2010, which vary considerably. This is the case for the decadal re-forecast experiment and to an even larger extent the case for the persistence and GCM historical experiments, which have a larger variation in mean absolute error. Overall, for the decade 2000-2010, we see good to reasonable

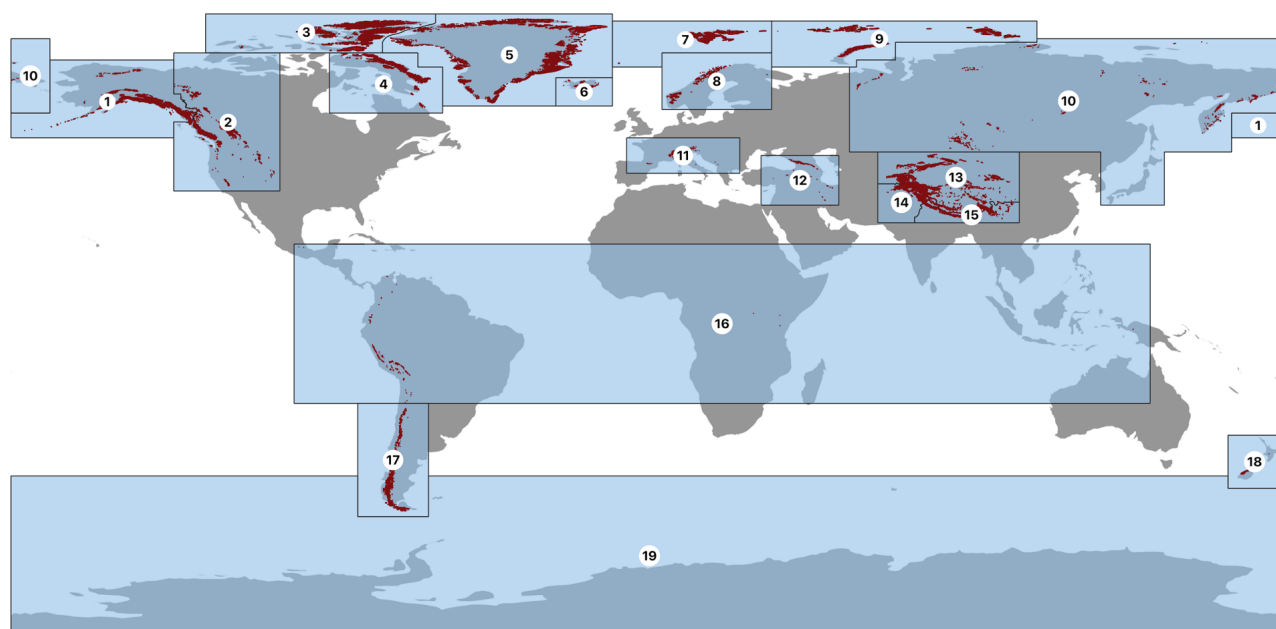


**Figure 3.** Map of all RGI regions, of which we use 18 in OGGM as we exclude Antarctica (region 19). Numbered light blue polygons correspond to the glacier regions (GTN-G, 2023) listed in Table 4 and Table 5. Dark red areas correspond to all glaciers listed in the RGI inventory (RGI Consortium, 2017). The country outlines are made with Natural Earth country polygons (<https://www.naturalearthdata.com>, last access: 02 January 2024).

fit between observed and simulated mean mass balances. For the decadal re-forecast experiment, for ten out of 18 RGI regions, we see good fit (defined as a difference between regional means  $\leq 0.1$  m w.e.) between simulated and observed regional mean specific mass balances. For seven out of 18 regions, we see reasonable fit (difference between regional means 0.1 – 0.3 m w.e.) and for one region, we observe mediocre fit (difference between regional means  $\geq 0.3$  m w.e.). These differences all lie within one standard deviation from the mean, for the simulations as well as within the mean error of observations (Hugonnet et al., 2021). All 2000-2010 observed values and their uncertainty, as well as all simulated values per experiment are included in Table 3.

The 2010-2020 results for the other two experiments are slightly different than for the 2000-2010 period, in that the persistence experiment outperforms the decadal re-forecast experiment in overall skill score. The mean absolute error for the decadal re-forecast experiment is at  $0.28 \pm 0.24$  m w.e., while persistence mean absolute error is  $0.24 \pm 0.20$  m w.e., at Pearson correlation coefficients of 0.69 and 0.77 respectively. In terms of goodness of fit per region however, the decadal re-forecast experiment slightly outperforms the persistence experiment, with 11 of 18 regions showing good fit (defined as a difference



**Table 3.** Observed and simulated WGMS mass balance skill scores. Summary of the comparison between WGMS observed and simulated mass balances for all three experiments and the decades 2000-2010 and 2010-2020. The statistics shown are ME: model error, MAE: mean absolute error and Pearson correlation, as well as 1 standard deviation from the mean of the particular statistic.

Skill Measure	Decadal RF	Persistence	GCM Historical
2000-2010			
ME (m w.e.)	0.082 ± 0.31	0.24 ± 0.33	0.18 ± 0.33
MAE (m w.e.)	0.28 ± 0.23	0.35 ± 0.26	0.33 ± 0.25
Pearson <i>r</i>	0.71 ± 0.22	0.64 ± 0.19	0.65 ± 0.23
2010-2020			
ME (m w.e.)	-0.043 ± 0.33	-0.098 ± 0.27	-0.069 ± 0.35
MAE (m w.e.)	0.28 ± 0.24	0.24 ± 0.20	0.31 ± 0.26
Pearson <i>r</i>	0.69 ± 0.17	0.77 ± 0.12	0.66 ± 0.10

between regional means  $\leq 0.1$  m w.e.). Five of 18 regions show reasonable fit (difference between regional means 0.1 – 0.3 m w.e.) and two regions show mediocre fit (difference between regional means  $\geq 0.3$  m w.e.). The persistence experiment shows 8 regions with good fit, 8 regions with reasonable fit and two regions with mediocre fit. The exact goodness of fit numbers, including the observations and observational uncertainty can be found in Table 5.

315 The fact that the persistence experiment performs markedly better for this decade than for the previous one, while skill scores and goodness of fit are similar for the decadal re-forecast experiment, could lie in the calibration. As explained in Sect. 2.2.2, the calibration and validation periods are the same. Because of the nature of persistence forecasts, the forcing data for the 2000-2010 period originated from 1990–2000, and was not used in calibration. For the period 2010-2020, however, both the climate data for the persistence forecast (2000-2010) and the forecasted decade were part of the calibration, resulting in a  
 320 bias of 0 for the full time period 2000–2020. To assess the effect of this, we run another persistence simulation, this time with a model only calibrated for the period 2000-2010, leaving 2010-2020 for validation. This is also the scenario that would occur when using persistence to forecast 2020-2030: the model is calibrated for the decade prior to the forecasted one. This leads to a markedly worse score for the persistence forecast, with a mean absolute error of  $0.38 \pm 0.36$  m w.e. and a Pearson correlation coefficient of 0.26, indicating low correlation.

325 On the whole, the global skill displayed in the decadal re-forecast experiment is comparable to or slightly better than the other experiments. Especially with warming and glacier mass loss accelerating (Hugonnet et al., 2021), this is an argument for forcing near-term simulation with initialized forecasts over persistence forecasts, which lack the warming trend over the simulation period. The choice of initialized forecast forcing over uninitialized projections stems mainly from the probabilistic context: projections, especially as SSP differences increase over time, are inherently more uncertain than a forecast initialized  
 330 at the beginning of the forecast period. Despite these advantages, decadal forecasts are far from perfect, and the continuation of projects such as the DCP contribution to CMIP6 (Boer et al., 2016) is essential to ensure their operational use. In fact,

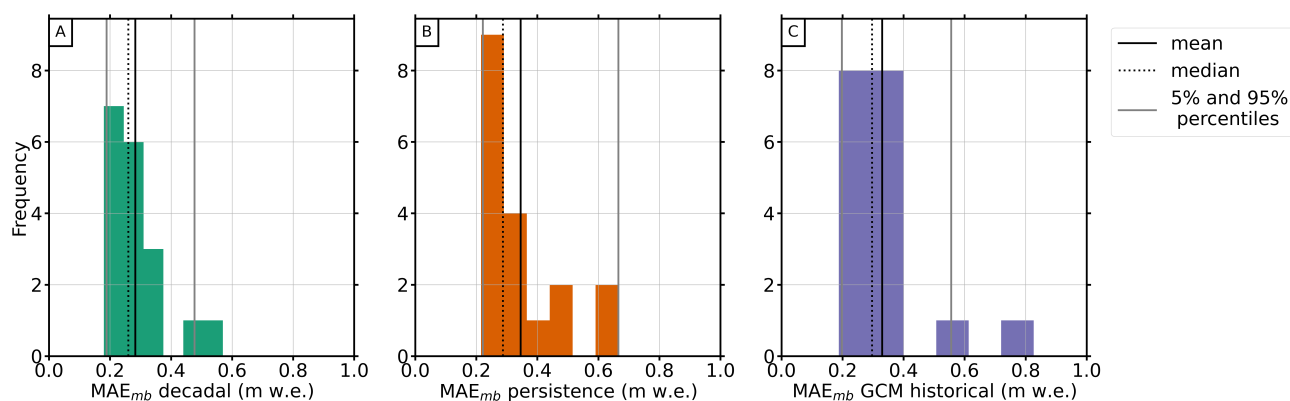


**Figure 4.** Mean absolute error for runs with decadal forcing (a), persistence forcing (b) and GCM historical forcing (c), for all RGI regions (N = 18). The vertical lines indicate mean (bold, black), median (dotted, black) and 5th and 95th percentiles (grey) of the mean absolute error.

re-forecast quality, meaning the degree of correspondence between observed and simulated temperature and precipitation, could in part explain the regional differences in goodness of fit. We refer to Delgado-Torres et al. (2022) for a comprehensive analysis of quality of the re-forecasts used here. Their analysis shows generally high skill for DCPD forecasts of temperature, especially over land masses. For precipitation however, skill is limited in several regions, including central Europe (region 11) and Western Canada/ US (region 2), which show the least skill out of all regions (see Table 4 and Table 5). Good precipitation skill is observed for northern Europe and Central Asia, in line with our yielded ‘good fit’ results for Svalbard and Jan Mayen (region 7) and Central Asia (region 13). It is likely that precipitation forecasts are a limiting factor in mass balance modelling on the global scale, which is to be kept in mind when designing future studies.

### 3.3 Observed Data Differences

Finally, this study clearly benefits from the availability of two separate data sets of observed mass balance for the same 2000–2020 time period. This not only allows for more critical assessment of model results, but also of uncertainty within observations. The use of both data sets here warrants a comparison between overlapping observations. For the period 2000–2010, we calculate the mean mass balance for all glaciers where the WGMS data set has full observations throughout the decade (N = 90). For this subset of 90 glaciers, we find a mean bias/difference of -0.049 m w.e. and an absolute bias/difference of 0.23 m w.e. between the WGMS and geodetic mass balance data. For the period 2010–2020 we have 100 glaciers with uninterrupted mass balance coverage from the WGMS data set. Comparing to the Hugonnet et al. (2021) mean mass balances yields a mean bias/difference of -0.15 m w.e. and an absolute bias/difference of 0.32 m w.e.. For the full time period 2000–2020, a sub-set of 67 glacier has observations throughout the full time period. The mean bias/difference here is -0.11 m w.e. and the absolute bias/difference is 0.23 m w.e.. These results are along the same magnitude of error we observe when comparing our decadal re-forecast





**Table 4.** Color-coded overview of mass balances over the period 2000–2010, from the decadal re-forecast, persistence and GCM historical experiments, as well as observed data from Hugonnet et al. (2021). The Hugonnet et al. (2021) values include their uncertainties. The table is color coded according to goodness of fit between experiment and Hugonnet et al. (2021) data: blue labels indicate a good fit (difference between regional means  $\leq 0.1$  m w.e.), yellow a reasonable fit (difference between regional mean 0.1-0.3 m w.e.) and red labels indicate mediocre fit (difference between regional mean  $\geq 0.3$  m w.e.).

RGI Region	Mean mass balance 2000-2010 (m w.e.)			
	Observed (Hugonnet et al., 2021)	Decadal re-forecast	Persistence	GCM Historical
1 Alaska	-0.29 ± 0.47	-0.34	-0.28	-0.0055
2 Western Canada / US	-0.18 ± 0.48	-0.42	-0.10	-0.077
3 Arctic Canada North	-0.35 ± 0.28	-0.11	-0.062	-0.0024
4 Arctic Canada South	-0.40 ± 0.37	-0.32	-0.13	-0.16
5 Greenland Periphery	-0.34 ± 0.38	-0.28	0.31	0.10
6 Iceland	-0.42 ± 0.35	-0.57	-0.056	-0.22
7 Svalbard and Jan Mayen	-0.26 ± 0.28	-0.18	-0.0089	-0.10
8 Scandinavia	-0.46 ± 0.45	-0.22	0.044	-0.41
9 Russian Arctic	-0.31 ± 0.26	-0.23	-0.083	-0.13
10 North Asia	-0.38 ± 0.58	-0.42	-0.27	-0.27
11 Central Europe	-0.60 ± 0.62	-0.36	0.040	0.21
12 Caucasus/ Middle East	-0.35 ± 0.50	-0.35	-0.070	-0.27
13 Central Asia	-0.21 ± 0.46	-0.16	-0.054	-0.11
14 South Asia West	-0.08 ± 0.48	-0.09	0.048	-0.033
15 South Asia East	-0.34 ± 0.48	-0.13	-0.25	-0.30
16 Low Latitudes	-0.33 ± 0.49	-0.34	-0.41	-0.37
17 Southern Andes	-0.17 ± 0.56	-0.09	-0.17	-0.053
18 New Zealand	-0.060 ± 0.61	-0.15	0.13	-0.18

simulation results to observations, as well as the uncertainties associated with the Hugonnet et al. (2021) data. This reinforces the need for caution when interpreting observations but also confirms the satisfactory quality of the simulated results.

#### 4 Conclusion and Outlook

Our results show that there is merit in using decadal scale forecasts in glacier modelling and they show good predictive skill of averaged multi-annual mass balances. We see that, indicated by lower errors and higher correlations, the use of decadal re-forecasts yields comparable or better results than forcing OGGM with a persistence forecast or the current state of the art: GCM historical data of temperature and precipitation. Globally, we see good or reasonable agreement between simulated



**Table 5.** Color-coded overview of mass balances over the period 2010–2020, from the decadal re-forecast, persistence and GCM historical/projection experiments, as well as observed data from Hugonnet et al. (2021). The Hugonnet et al. (2021) values include their uncertainties. The table is color coded according to goodness of fit between experiment and Hugonnet et al. (2021) data: blue labels indicate a good fit (difference between regional means  $\leq 0.1$  m w.e.), yellow a reasonable fit (difference between regional mean 0.1-0.3 m w.e.) and red labels indicate mediocre fit (difference between regional mean  $\geq 0.3$  m w.e.).

RGI Region	Mean mass balance 2010-2020 (m w.e.)			
	Observed (Hugonnet et al., 2021)	Decadal re-forecast	Persistence	GCM Historical and Projection
1 Alaska	-0.57 ± 0.45	-0.51	-0.32	-0.34
2 Western Canada / US	-0.50 ± 0.51	-0.58	-0.23	-0.45
3 Arctic Canada North	-0.40 ± 0.27	-0.21	-0.36	-0.23
4 Arctic Canada South	-0.45 ± 0.35	-0.58	-0.37	-0.51
5 Greenland Periphery	-0.22 ± 0.36	-0.41	-0.38	-0.37
6 Iceland	-0.25 ± 0.33	-0.56	-0.43	-0.51
7 Svalbard and Jan Mayen	-0.30 ± 0.27	-0.32	-0.23	-0.22
8 Scandinavia	-0.36 ± 0.44	-0.46	-0.40	-0.58
9 Russian Arctic	-0.29 ± 0.23	-0.39	-0.29	-0.26
10 North Asia	-0.44 ± 0.59	-0.53	-0.39	-0.50
11 Central Europe	-0.59 ± 0.63	-0.58	-0.39	-0.54
12 Caucasus/ Middle East	-0.58 ± 0.54	-0.58	-0.27	-0.76
13 Central Asia	-0.27 ± 0.47	-0.28	-0.16	-0.32
14 South Asia West	-0.14 ± 0.47	-0.046	-0.08	-0.23
15 South Asia East	-0.49 ± 0.49	-0.11	-0.38	-0.52
16 Low Latitudes	-0.32 ± 0.49	-0.69	-0.25	-0.96
17 Southern Andes	-0.28 ± 0.34	-0.28	-0.022	-0.31
18 New Zealand	-0.34 ± 0.65	-0.41	-0.03	-0.45

and observed mean mass balances for almost all RGI regions, and on a glacier-to-glacier basis. The decadal re-forecasts are able to reliably predict mean cumulative mass balance over single decades for the WGMS set of reference glaciers, providing an important basis for modelling the amount of mass moving downstream over a decade. This, of course, operates on the assumption that real time decadal forecasts (for decades that lie in the future) and GCM projections would be of similar quality to the re-forecasts and historical runs used in the current study, and would benefit from future validation. The use of decadal forecasts would not replace GCM projections for 21<sup>st</sup> century glacier modelling, but can provide added clarity on the near-term, especially in terms of uncertainty. An important benefit of initialized forecasts on the decadal scale is their narrower distribution compared to uninitialized scenario projections. Especially as the SSPs drift apart over the years, more uncertainty is introduced as we progress in time. Also Payne et al. (2022) note in their assessment of forcing with decadal re-forecasts vs.



uninitialized projections that there is an established demand for communicating both likely values and uncertainty of a forecast made with an impact model (Bruno Soares and Dessai, 2016). When the effort is to minimize this uncertainty and make a forecast as precise as possible, forcing with initialized forecasts is likely preferable on the decadal scale. The benefit over using persistence forecasts may also become more marked, as climate change will likely increase decadal climate variability (Nijse et al., 2019), and thus differences in climate between separate decades.

The results shown here are limited by multiple factors and we especially highlight the need for continuing this research with a larger ensemble, which could increase predictive skill (Smith et al., 2013). Another important step towards applications in hydrology and industry would be the use of decadal forecasts to force OGGM dynamically, as opposed to the static mass balance in the current study. This would mainly serve to ensure a more accurate initial state of the glacier, important for areas where glaciers have already changed significantly since their RGI inventory date, such as the European Alps.

Finally, the foremost aim when continuing this research is to have the highest possible quality near-term glacier simulations for the next decade. Accurate knowledge of near-term trends is essential, as these time scales are most relevant for applications in hydrology and industry (Frans et al., 2016; Lane and Nienow, 2019), especially in regions where populations are directly affected in the form of water scarcity or flooding. This would add to a growing database of field cases utilizing near-term forecasts, see e.g. O’Kane et al. (2023). Our results support the case for using decadal forecasts to achieve this, rather than depending only on the continuation of inter-decadal trends. The next applications of the methods laid out in this study would be on basin- and global scales, forcing OGGM with a multi-model ensemble of decadal forecasts, into the 2030s. OGGM would be applied to acquire decadal estimates of future mean and cumulative mass balance, volume and area change as well as glacier runoff. Results could provide robust, important information on the amount of glacier mass lost and moving downstream in the form of runoff. With the continuing and accelerating impacts of climate change on glaciers and water resources, we emphasize the need for these near-term predictions, in order to best inform and protect the communities dependent on them.

*Code and data availability.* All OGGM source code is available via <https://github.com/OGGM>, with documentation available at <https://docs.oggm.org/en/v1.5.3/>. All decadal re-forecast and GCM data is available via <https://esgf-node.llnl.gov/search/cmip6/>. The OGGM baseline climate CRU is available in the OGGM pre-processed directories [https://cluster.klima.uni-bremen.de/~oggm/gdirs/oggm\\_v1.4/exps/CRU\\_new/elev\\_bands/qc0/pcp2.5/match\\_geod\\_pergla](https://cluster.klima.uni-bremen.de/~oggm/gdirs/oggm_v1.4/exps/CRU_new/elev_bands/qc0/pcp2.5/match_geod_pergla).

*Author contributions.* LL helped conceive the study, co-developed the drift correction, did the analysis and wrote the paper. AV ran the global simulations and improved writing and general study design. AAS contributed to the study design and development of the drift correction. FM is the main developer of OGGM and contributed to study design, model set-up and improving the text. KF set up the original study concept and contributed to discussions and improving writing.

<https://doi.org/10.5194/egusphere-2024-387>

Preprint. Discussion started: 22 March 2024

© Author(s) 2024. CC BY 4.0 License.



*Competing interests.* The authors declare that no competing interests are present.

*Acknowledgements.* LL, employed by the project Global glacier mass balance prediction on seasonal and decadal scale “GLISSADE”, was funded by the Deutsche Forschungsgemeinschaft (DFG, German Research Foundation), Grant No. 416069075 (FO1269/1). AV was funded by the Austrian Science Fund (FWF) project P30256 and the German Research Foundation (DFG) – MA 6966/5-1. AAS was supported by 400 the Met Office Hadley Centre Climate Programme (HCCP) funded by the UK Department for Science, Innovation and Technology (DSIT). The authors would like to thank Dr. Mark Payne for the helpful discussion on decadal forecasting and Dr. Lizz Ultee for her encouragement while completing this study.



## References

- Allison, E. A.: The Spiritual Significance of Glaciers in an Age of Climate Change, *Wiley Interdisciplinary Reviews: Climate Change*, 6, 493–508, <https://doi.org/10.1002/wcc.354>, 2015.
- Bethke, I., Wang, Y., Counillon, F., Keenlyside, N., Kimmritz, M., Fransner, F., Samuelsen, A., Langehaug, H., Svendsen, L., Chiu, P.-G., Passos, L., Bentsen, M., Guo, C., Gupta, A., Tjiputra, J., Kirkevåg, A., Olivić, D., Seland, Ø., Solsvik Vågane, J., Fan, Y., and Eldevik, T.: NorCPM1 and its Contribution to CMIP6 DCP, *Geoscientific Model Development*, 14, 7073–7116, <https://doi.org/10.5194/gmd-14-7073-2021>, 2021.
- 410 Boer, G. J., Smith, D. M., Cassou, C., Doblas-Reyes, F., Danabasoglu, G., Kirtman, B., Kushnir, Y., Kimoto, M., Meehl, G. A., Msadek, R., Mueller, W. A., Taylor, K. E., Zwiers, F., Rixen, M., Ruprich-Robert, Y., and Eade, R.: The Decadal Climate Prediction Project (DCPP) Contribution to CMIP6, *Geoscientific Model Development*, 9, 3751–3777, <https://doi.org/10.5194/gmd-9-3751-2016>, 2016.
- Bosson, J. B., Huss, M., and Osipova, E.: Disappearing World Heritage Glaciers as a Keystone of Nature Conservation in a Changing Climate, *Earth's Future*, 7, 469–479, <https://doi.org/https://doi.org/10.1029/2018EF001139>, 2019.
- 415 Bruno Soares, M. and Dessai, S.: Barriers and enablers to the use of seasonal climate forecasts amongst organisations in Europe, *Climatic Change*, 137, 89–103, <https://doi.org/10.1007/s10584-016-1671-8>, 2016.
- Counillon, F., Keenlyside, N., Bethke, I., Wang, Y., Billeau, S., Shen, M. L., and Bentsen, M.: Flow-dependent assimilation of sea surface temperature in isopycnal coordinates with the Norwegian Climate Prediction Model, *Tellus A: Dynamic Meteorology and Oceanography*, 68, 32 437, <https://doi.org/10.3402/tellusa.v68.32437>, 2016.
- 420 Delgado-Torres, C., Donat, M. G., Gonzalez-Reviriego, N., Caron, L.-P., Athanasiadis, P. J., Bretonnière, P.-A., Dunstone, N. J., Ho, A.-C., Nicoli, D., Pankatz, K., et al.: Multi-model forecast quality assessment of CMIP6 decadal predictions, *Journal of Climate*, 35, 4363–4382, <https://doi.org/10.5194/egusphere-egu22-13156>, 2022.
- Dunstone, N., Lockwood, J., Solaraju-Murali, B., Reinhardt, K., Tsartsali, E. E., Athanasiadis, P. J., Bellucci, A., Brookshaw, A., Caron, L.-P., Doblas-Reyes, F. J., Früh, B., González-Reviriego, N., Gualdi, S., Hermanson, L., Materia, S., Nicodemou, A., Nicoli, D., Pankatz, K., 425 Paxian, A., Scaife, A., Smith, D., and Thornton, H. E.: Towards Useful Decadal Climate Services, *Bulletin of the American Meteorological Society*, <https://doi.org/10.1175/bams-d-21-0190.1>, 2022.
- Eis, J., Van der Laan, L., Maussion, F., and Marzeion, B.: Reconstruction of past glacier changes with an ice-flow glacier model: Proof of concept and validation, *Frontiers in Earth Science*, 9, 595 755, <https://doi.org/10.3389/feart.2021.595755>, 2021.
- Farinotti, D., Huss, M., Fürst, J. J., Landmann, J., Machguth, H., Maussion, F., and Pandit, A.: A consensus estimate for the ice thickness 430 distribution of all glaciers on Earth, *Nature Geoscience*, 12, 168–173, <https://doi.org/10.1038/s41561-019-0300-3>, 2019.
- Farinotti, D., Immerzeel, W. W., de Kok, R. J., Quincey, D. J., and Dehecq, A.: Manifestations and Mechanisms of the Karakoram Glacier Anomaly, *Nature Geoscience*, 13, 8–16, <https://doi.org/10.1038/s41561-019-0513-5>, 2020.
- Frans, C., Istanbuloglu, E., Lettenmaier, D. P., Clarke, G., Bohn, T. J., and Stumbaugh, M.: Implications of Decadal to Century Scale Glacio-hydrological Change for Water Resources of the Hood River Basin, OR, USA, *Hydrological Processes*, 30, 4314–4329, 435 <https://doi.org/10.1002/hyp.10872>, 2016.
- Frederikse, T., Landerer, F., Caron, L., Adhikari, S., Parkes, D., Humphrey, V. W., Dangendorf, S., Hogarth, P., Zanna, L., Cheng, L., et al.: The causes of sea-level rise since 1900, *Nature*, 584, 393–397, <https://doi.org/10.5194/egusphere-egu2020-7907>, 2020.



- Förster, K. and van der Laan, L. N.: A review on observed historical changes in hydroclimatic extreme events over Europe, in: *Climate Impacts on Extreme Weather*, edited by Ongoma, V. and Tabari, H., pp. 131–144, Elsevier, <https://doi.org/10.1016/B978-0-323-88456-440>, 3.00015-0, 2022.
- Förster, K., Hanzer, F., Stoll, E., Scaife, A. A., MacLachlan, C., Schöber, J., Huttenlau, M., Achleitner, S., and Strasser, U.: Retrospective forecasts of the upcoming winter season snow accumulation in the Inn headwaters (European Alps), *Hydrology and Earth System Sciences*, 22, 1157–1173, <https://doi.org/10.5194/hess-2017-370-rc1>, 2018.
- Goosse, H., Barriat, P.-Y., Dalaiden, Q., Klein, F., Marzeion, B., Maussion, F., Pelucchi, P., and Vlug, A.: Testing the consistency between changes in simulated climate and Alpine glacier length over the past millennium, *Climate of the Past*, 14, 1119–1133, <https://doi.org/10.5194/cp-14-1119-2018>, 2018.
- 445 GTN-G: GTN-G Glacier Regions. Global Terrestrial Network for Glaciers, <https://doi.org/10.5904/gtng-glacreg-2023-0>, 2023.
- Hargreaves, J. C.: Skill and uncertainty in climate models, *Wiley Interdisciplinary Reviews: Climate Change*, 1, 556–564, <https://doi.org/10.1002/wcc.58>, 2010.
- 450 Harris, I., Jones, P. D., Osborn, T. J., and Lister, D. H.: Updated High-resolution Grids of Monthly Climatic Observations - the CRU TS3.10 Dataset, *International Journal of Climatology*, 34, 623–642, <https://doi.org/10.1002/joc.3711>, 2014.
- Harris, I., Osborn, T. J., Jones, P., and Lister, D.: Version 4 of the CRU TS Monthly High-resolution Gridded Multivariate Climate Dataset, *Scientific Data*, 7, 1–18, <https://doi.org/10.1038/s41597-020-0453-3>, 2020.
- Hermanson, L., Smith, D., Seabrook, M., Bilbao, R., Doblas-Reyes, F., Tourigny, E., Lapin, V., Kharin, V. V., Merryfield, W. J., Sospedra-Alfonso, R., et al.: WMO global annual to decadal climate update: a prediction for 2021–25, *Bulletin of the American Meteorological Society*, 103, E1117–E1129, <https://doi.org/10.18356/9789210027939>, 2022.
- 455 Hock, R., Bliss, A., Marzeion, B. E. N., Giesen, R. H., Hirabayashi, Y., Huss, M., Radic, V., and Slangen, A. B.: GlacierMIP - A Model Intercomparison of Global-scale Glacier Mass-balance Models and Projections, *Journal of Glaciology*, 65, 453–467, <https://doi.org/10.1017/jog.2019.22>, 2019.
- 460 Hossain, M. M., Garg, N., Anwar, A. F., Prakash, M., and Bari, M.: Intercomparison of drift correction alternatives for CMIP5 decadal precipitation, *International Journal of Climatology*, 42, 1015–1037, <https://doi.org/10.1002/joc.7287>, 2022.
- Hugonnet, R., McNabb, R., Berthier, E., Menounos, B., Nuth, C., Girod, L., Farinotti, D., Huss, M., Dussailant, I., Brun, F., et al.: Accelerated global glacier mass loss in the early twenty-first century, *Nature*, 592, 726–731, <https://doi.org/10.1038/s41586-021-03436-z>, 2021.
- Huss, M. and Hock, R.: Global-scale hydrological response to future glacier mass loss, *Nature Climate Change*, 8, 135–140, <https://doi.org/10.1038/s41558-017-0049-x>, 2018.
- 465 Huston, A., Siler, N., Roe, G. H., Pettit, E., and Steiger, N. J.: Understanding Drivers of Glacier-length Variability Over the Last Millennium, *The Cryosphere*, 15, 1645–1662, <https://doi.org/10.5194/tc-15-1645-2021>, 2021.
- Immerzeel, W. W., Lutz, A. F., Andrade, M., Bahl, A., Biemans, H., Bolch, T., Hyde, S., Brumby, S., Davies, B., Elmore, A., et al.: Importance and vulnerability of the world’s water towers, *Nature*, 577, 364–369, <https://doi.org/10.1038/s41586-019-1822-y>, 2020.
- 470 Jansson, P., Hock, R., and Schneider, T.: The Concept of Glacier Storage: a Review, *Journal of Hydrology*, 282, 116–129, [https://doi.org/10.1016/S0022-1694\(03\)00258-0](https://doi.org/10.1016/S0022-1694(03)00258-0), 2003.
- Kadow, C., Illing, S., Kröner, I., Ulbrich, U., and Cubasch, U.: Decadal climate predictions improved by ocean ensemble dispersion filtering, *Journal of Advances in Modeling Earth Systems*, 9, 1138–1149, <https://doi.org/10.1002/2016ms000787>, 2017.



- 475 Kataoka, T., Tatebe, H., Koyama, H., Mochizuki, T., Ogochi, K., Naoe, H., Imada, Y., Shiogama, H., Kimoto, M., and Watanabe, M.: Seasonal to Decadal Predictions with MIROC6: Description and Basic Evaluation, *Journal of Advances in Modeling Earth Systems*, 12, <https://doi.org/10.1029/2019MS002035>, 2020.
- Khari, V. V., Boer, G. J., Merryfield, W. J., Scinocca, J. F., and Lee, W. S.: Statistical Adjustment of Decadal Predictions in a Changing Climate, *Geophysical Research Letters*, 39, <https://doi.org/10.1029/2012GL052647>, 2012.
- 480 Kiem, A. S. and Verdon-Kidd, D. C.: Steps Toward "Useful" Hydroclimatic Scenarios for Water Resource Management in the Murray-Darling Basin, *Water Resources Research*, 47, <https://doi.org/10.1029/2010wr009803>, 2011.
- Kozioł, C. P. and Arnold, N.: Modelling Seasonal Meltwater Forcing of the Velocity of Land-terminating Margins of the Greenland Ice Sheet, *The Cryosphere*, 12, 971–991, <https://doi.org/10.5194/tc-12-971-2018>, 2018.
- Kushnir, Y., Scaife, A. A., Arritt, R., Balsamo, G., Boer, G., Doblas-Reyes, F., Hawkins, E., Kimoto, M., Kolli, R. K., Kumar, A., et al.: Towards operational predictions of the near-term climate, *Nature Climate Change*, 9, 94–101, <https://doi.org/10.1038/s41558-018-0359-7>, 485 2019.
- Lane, S. N. and Nienow, P. W.: Decadal-Scale Climate Forcing of Alpine Glacial Hydrological Systems., *Water Resources Research*, 55, 2478–2492, <https://doi.org/10.1029/2018WR024206>, 2019.
- Malles, J.-H. and Marzeion, B.: Twentieth century global glacier mass change: an ensemble-based model reconstruction, *The Cryosphere*, 15, 3135–3157, <https://doi.org/10.5194/tc-15-3135-2021>, 2021.
- 490 Marzeion, B., Jarosch, A., and Hofer, M.: Past and future sea-level change from the surface mass balance of glaciers, *The Cryosphere*, 6, 1295–1322, <https://doi.org/10.5194/tc-6-1295-2012>, 2012.
- Marzeion, B., Champollion, N., Haeberli, W., Langley, K., Leclercq, P., and Paul, F.: Observation-based estimates of global glacier mass change and its contribution to sea-level change, *Integrative study of the mean sea level and its components*, pp. 107–132, <https://doi.org/10.1007/s10712-016-9394-y>, 2017.
- 495 Maussion, F., Butenko, A., Champollion, N., Dusch, M., Julia Eis, K. F., Gregor, P., Jarosch, A. H., Landmann, J., Oesterle, F., Recinos, B., Rothenpieler, T., Vlug, A., Wild, C. T., and Marzeion, B.: The Open Global Glacier Model (OGGM) v1.1, *Geoscientific Model Development*, 2019, 909–931, <https://doi.org/10.5194/gmd-12-909-2019>, 2019.
- Merryfield, W. J., Baehr, J., Batté, L., Becker, E. J., Butler, A. H., Coelho, C. A., Danabasoglu, G., Dirmeyer, P. A., Doblas-Reyes, F. J., Domeisen, D. I., et al.: Current and emerging developments in subseasonal to decadal prediction, *Bulletin of the American Meteorological* 500 *Society*, 101, E869–E896, <https://doi.org/10.1175/BAMS-D-19-0037.1>, 2020.
- New, M., Lister, D., Hulme, M., and Makin, I.: A high-resolution data set of surface climate over global land areas, *Climate Research*, 21, 1–25, <https://doi.org/10.3354/cr021001>, 2002.
- Nijssen, F. J., Cox, P. M., Huntingford, C., and Williamson, M. S.: Decadal Global Temperature Variability Increases Strongly with Climate Sensitivity, *Nature Climate Change*, 9, 598–601, <https://doi.org/10.1038/s41558-019-0527-4>, 2019.
- 505 O’Kane, T. J., Scaife, A. A., Kushnir, Y., Brookshaw, A., Buontempo, C., Carlin, D., Connell, R. K., Doblas-Reyes, F., Dunstone, N., Förster, K., Graça, A., Hobday, A. J., Kitsios, V., van der Laan, L., Lockwood, J., Merryfield, W. J., Paxian, A., Payne, M. R., Reader, M. C., Saville, G. R., Smith, D., Solaraju-Murali, B., Caltabiano, N., Carman, J., Hawkins, E., Keenlyside, N., Kumar, A., Matei, D., Pohlmann, H., Power, S., Raphael, M., Sparrow, M., and Wu, B.: Recent applications and potential of near-term (interannual to decadal) climate predictions, *Frontiers in Climate*, 5, <https://doi.org/10.3389/fclim.2023.1121626>, 2023.
- 510 Payne, M. R., Danabasoglu, G., Keenlyside, N., Matei, D., Miesner, A. K., Yang, S., and Yeager, S. G.: Skilful decadal-scale prediction of fish habitat and distribution shifts, *Nature Communications*, 13, 2660, <https://doi.org/10.1038/s41467-022-30280-0>, 2022.





- Pfeffer, W. T., Arendt, A. A., Bliss, A., Bolch, T., Cogley, J. G., Gardner, A. S., and Consortium, . . R.: The Randolph Glacier Inventory: A Globally Complete Inventory of Glaciers, *Journal of glaciology*, 60, 537–552, <https://doi.org/10.3189/2014JoG13J176>, 2014.
- Ramírez Villegas, J. and Jarvis, A.: Downscaling global circulation model outputs: the delta method decision and policy analysis Working Paper No. 1., 2010.
- 515 Recinos, B., Maussion, F., Rothenpieler, T., and Marzeion, B.: Impact of frontal ablation on the ice thickness estimation of marine-terminating glaciers in Alaska, *The Cryosphere*, 13, 2657–2672, <https://doi.org/10.5194/tc-13-2657-2019>, 2019.
- RGI Consortium: Randolph Glacier Inventory (RGI) – A Dataset of Global Glacier Outlines: Version 6.0. Technical Report, Global Land Ice Measurements from Space, <https://doi.org/10.7265/N5-RGI-60>, 2017.
- 520 Risbey, J. S., Squire, D. T., Black, A. S., DelSole, T., Lepore, C., Matear, R. J., Monselesan, D. P., Moore, T. S., Richardson, D., Schepen, A., et al.: Standard assessments of climate forecast skill can be misleading, *Nature Communications*, 12, 4346, <https://doi.org/10.1038/s41467-021-23771-z>, 2021.
- Roe, G. H., Christian, J. E., and Marzeion, B.: On the Attribution of Industrial-Era Glacier Mass Loss to Anthropogenic Climate Change, *The Cryosphere*, 15, 1889–1905, <https://doi.org/10.5194/tc-15-1889-2021>, 2021.
- 525 Rounce, D. R., Hock, R., Maussion, F., Hugonnet, R., Kochtitzky, W., Huss, M., Berthier, E., Brinkerhoff, D., Compagno, L., Copland, L., et al.: Global glacier change in the 21st century: Every increase in temperature matters, *Science*, 379, 78–83, <https://doi.org/10.1126/science.abo1324>, 2023.
- Réveillet, M., Six, D., Vincent, C., Rabatel, A., Dumont, M., Lafaysse, M., Morin, S., Vionnet, V., and Litt, M.: Relative Performance of Empirical and Physical Models in Assessing the Seasonal and Annual Glacier Surface Mass Balance of Saint-Sorlin Glacier (French Alps), *The Cryosphere*, 12, 1367–1386, <https://doi.org/https://doi.org/10.5194/tc-12-1367-2018>, 2018.
- 530 Slangen, A., Adloff, F., Jevrejeva, S., Leclercq, P., Marzeion, B., Wada, Y., and Winkelmann, R.: A review of recent updates of sea-level projections at global and regional scales, *Integrative Study of the Mean Sea level and Its Components*, pp. 395–416, [https://doi.org/10.1007/978-3-319-56490-6\\_17](https://doi.org/10.1007/978-3-319-56490-6_17), 2017.
- Smith, D. M., Eade, R., and Pohlmann, H.: A comparison of full-field and anomaly initialization for seasonal to decadal climate prediction, *Climate Dynamics*, 41, 3325–3338, <https://doi.org/10.1007/s00382-013-1683-2>, 2013.
- 535 Solaraju-Murali, B., Bojovic, D., Gonzalez-Reviriego, N., Nicodemou, A., Terrado, M., Caron, L. P., and Doblus-Reyes, F. J.: How Decadal Predictions Entered the Climate Services Arena: An Example from the Agriculture Sector, *Climate Services*, 27, 100303, <https://doi.org/10.1016/j.cliser.2022.100303>, 2022.
- Tatebe, H., Ogura, T., Nitta, T., Komuro, Y., Ogochi, K., Takemura, T., Sudo, K., Sekiguchi, M., Abe, M., Saito, F., Chikira, M., Watanabe, S., Mori, M., Hirota, N., Kawatani, Y., Mochizuki, T., Yoshimura, K., Takata, K., O’ishi, R., Yamazaki, D., Suzuki, T., Kurogi, M., Kataoka, T., Watanabe, M., and Kimoto, M.: Description and Basic Evaluation of Simulated Mean State, Internal Variability, and Climate Sensitivity in MIROC6, *Geoscientific Model Development*, 12, 2727–2765, <https://doi.org/10.5194/gmd-12-2727-2019>, 2019.
- 540 Ultee, L., Coats, S., and Mackay, J.: Glacial runoff buffers droughts through the 21st century, *Earth System Dynamics*, 13, 935–959, <https://doi.org/10.5194/esd-13-935-2022>, 2022.
- 545 Vargo, L. J., Anderson, B. M., Dadić, R., Horgan, H. J., Mackintosh, A. N., King, A. D., and Lorrey, A. M.: Anthropogenic warming forces extreme annual glacier mass loss, *Nature Climate Change*, 10, 856–861, <https://doi.org/10.26686/wgtn.14658585.v1>, 2020.
- WGMS: Reference Glaciers for Mass Balance, [https://wgms.ch/products\\_ref\\_glaciers/](https://wgms.ch/products_ref_glaciers/), accessed: 2022-12-01, 2022.
- Zekollari, H., Huss, M., and Farinotti, D.: On the Imbalance and Response Time of Glaciers in the European Alps, *Geophysical Research Letters*, 47, <https://doi.org/10.1029/2019GL085578>, 2020.



- 550 Zekollari, H., Huss, M., Farinotti, D., and Lhermitte, S.: Ice-Dynamical Glacier Evolution Modeling—A Review, *Reviews of Geophysics*, 60, <https://doi.org/10.1029/2021rg000754>, 2022.
- Zhou, T., Wang, B., Yu, Y.-Q., Liu, Y., Zheng, W., Li, L., Wu, B., Lin, P., Guo, Z., Man, W., Bao, Q., Duan, A., Liu, H., Chen, X., He, B., Li, J., Zou, L., Wang, X., Zhang, L., and Zhang, W.: The FGOALS Climate System Model as a Modeling Tool for Supporting Climate Sciences: An Overview, *Earth and Planetary Physics*, 2, 276–291, <https://doi.org/10.26464/epp2018026>, 2018.
- 555 Zhu, E., Yuan, X., and Wood, A. W.: Benchmark decadal forecast skill for terrestrial water storage estimated by an elasticity framework, *Nature communications*, 10, 1237, <https://doi.org/10.1038/s41467-019-09245-3>, 2019.